Primary Results on Simulation of a New Kind Traveling Wave of Permanent Form *

Min CHEN†

Abstract

This talk concerns the nonlinear dispersive waves in a water channel. Results from the study of a new version of the classical Boussinesq model system for the two-way propagation of water waves will be presented. The talk will feature presentations about theoretical work, numerical analysis, implementation of numerical schemes and the use of these schemes to better understand the models, reports on laboratory experiments and comparisons of model predictions with real-world data. Some interesting simulations will be presented, which include a new set of traveling waves of permanent form, the generation of tidal waves and head-on collision of tidal waves.

1 Introduction

In this paper, we study the propagation of waves in a uniform horizontal channel of length L_0 filled to a depth h with an incompressible perfect fluid. Assuming the wave motion is generated irrotationally and that it is uniform across the width of the channel, the two-dimensional Euler equations are the full equations of motion. Since the numerical simulation of Euler equations are rather challenging and costly (cf. [1]), especially when a relative long time period is involved, further approximations are often made in practice. Assuming that the maximum deviation a of the free surface from its undisturbed position is small relative to h (small-amplitude waves), that the typical wavelength λ is large relative to h (long waves), and that the Ursell number $S = a\lambda^2/h^3$ is of order one, the Euler equations may be formally approximated by

$$\begin{aligned} \eta_t - \frac{1}{6}\eta_{xxt} &= -u_x - (u\eta)_x, \\ u_t - \frac{1}{6}u_{xxt} &= -\eta_x - uu_x, \end{aligned} \qquad \text{for (x,t)} \ \in \Omega = [0, L] \times [0, T], \tag{1}$$

where $L = L_0/h$, x is distance along the channel scaled by h, t is elapsed time scaled by $\sqrt{h/g}$ with g being the acceleration of gravity. The dependent variable η is such that $h(1 + \eta(x,t))$ is the total depth at location x at time t, and $u = u(x,t)$ is the horizontal velocity scaled by $c_0 = \sqrt{gh}$ at the water level $\sqrt{\frac{2}{3}}h$ at the location x along the channel at time t.

As pointed out in [4], the system (1) is formally equivalent and correct to the Boussinesq's original system (cf. [6]) through first order with regard to the small parameter

*This work was supported in part by NSF grant DMS-9622858 and DMS-9753216.

†Department of Mathematics, Penn State University, University Park, PA, 16802

$\epsilon = a/h$, and has the same formal status as the famous KdV equation which describe waves moving in one direction. Among a class of formally equivalent systems studied in [4], system (1) is particularly interesting because that the dispersive relation is stabilizing for all wave numbers and the natural initial-boundary-value problems that arise in laboratory experiments are well-posed, which is to say that when (1) is associated with the initial and boundary conditions

$$\begin{aligned} \eta(0,t) &= h_1(t), \quad \eta(L,t) = h_2(t), \quad \eta(x,0) = h_0(x), \\ u(0,t) &= v_1(t), \quad u(L,t) = v_2(t), \quad u(x,0) = v_0(x), \end{aligned} \tag{2}$$

which satisfy the consistency requirements

$$h_1(0) = h_0(0), \quad h_2(0) = h_0(L), \quad v_1(0) = v_0(0), \quad v_2(0) = v_0(L),$$

there exists an unique solution over a positive time interval and the solution is as regular as the initial and boundary data affords.

2 Numerical Scheme

In this section, we present the scheme which was shown in [2] to be fourth-order accurate both in time and in space, unconditional stable, and have optimal computational complexity, which is to say the operation cost per time step is of order M with M being the number of grid points in the spatial discretization.

The numerical scheme is based on the integral equations of (1). Inverting the operator $(1 - \frac{1}{6}\partial_x^2)$ subject to the boundary conditions in (2) and integrating the right-hand side by parts, one finds

$$\begin{aligned} \eta_t &= \int_0^L K(x,s)(u + \eta u)ds + S(L-x)h_1' + S(x)h_2', \\ u_t &= \int_0^L K(x,s)(\eta + \frac{1}{2}u^2)ds + S(L-x)v_1' + S(x)v_2', \end{aligned} \tag{3}$$

with

$$K(x,s) = \frac{1}{12}\big(S(L-x-s) + \mathrm{sign}(x-s)S(L-|x-s|)\big)$$

and

$$S(x) = \frac{\sinh(x/\sqrt{6})}{\sinh(L/\sqrt{6})}.$$

Let Δt be the step-size for the temporal discretization and Δx the length of the spatial discretization; let $(M+1)$ be the number of spatial mesh points, so that $M\Delta x = L$. The equations in (3) are first discretized in space via numerical quadrature; the resultant system of ordinary differential equations are then integrated forward in time by a finite-difference, predictor-corrector method.

<u>*Spatial Discretization*</u> The spatial discretization is effected by approximating $\phi(x_i) = \int_0^L K(x_i,s)y(s)ds$, $i = 0, 1, \cdots, M$. Using the trapezoidal rule with boundary corrections

and taking account of the fact that $K(x,s)$ is discontinuous at $x=s$, one has that

$$\begin{aligned}\phi(x_i) \approx &\frac{1}{2}\Delta x\Big[K_i(0)y(0) + (K_i(i\Delta x^-) + K_i(i\Delta x^+))y(i\Delta x) + K_i(L)y(L)\Big]\\ &+ \Delta x \sum_{j=1, j\neq i}^{M-1} K_i(j\Delta x)y(j\Delta x) + \frac{1}{12}\Delta x^2\Big[(K_i(s)y(s))'\,|_{0+}\\ &- (K_i(s)y(s))'\,|_{i\Delta x^-} + (K_i(s)y(s))'\,|_{i\Delta x^+} - (K_i(s)y(s))'\,|_{M\Delta x^-}\Big]\end{aligned}$$

where $K_i(s) = K(x_i, s)$. The derivatives $y'(i\Delta x)$, $i = 0, \cdots, M$, may be replaced by the second-order finite differences. Therefore $\phi(x_i)$ may be approximated by a function $\phi_i(\mathbf{y})$ where $\mathbf{y} = (y_0, \cdots, y_M)$ with $y_i = y(i\Delta x)$.

The semi-discrete algorithm of (3) is then to find vectors $\mathbf{n} = (n_0(t), \cdots, n_M(t))$ and $\mathbf{w} = (w_0(t), \cdots, w_M(t))$ which are approximations to η and u respectively, such that for $i = 1, \cdots, M-1$,

$$(4)\qquad \begin{aligned}(n_i)_t &= \phi_i(\mathbf{w} + \mathbf{n}\circ\mathbf{w}) + S(L - x_i)h_1' + S(x_i)h_2', \quad n_0 = h_1, \quad n_M = h_2,\\ (w_i)_t &= \phi_i(\mathbf{n} + \frac{1}{2}\mathbf{w}\circ\mathbf{w}) + S(L - x_i)v_1' + S(x_i)v_2', \quad w_0 = v_1, \quad w_M = v_2.\end{aligned}$$

The symbol $\mathbf{n}\circ\mathbf{w}$ denotes the component-wise product of $\mathbf{n}$ and $\mathbf{w}$, which is to say $\mathbf{n}\circ\mathbf{w} = (\eta_0 u_0, \cdots, \eta_M u_M)$.

If $M+1$ is the number of spatial mesh points, a direct evaluation of $\phi_i(\mathbf{y})$, $i = 0, 1, \cdots, M$, will involve on the order of M^2 operations. To reduce the computation to order M operations, an acceleration technique which was put forward in [3] and [2] is used in the computation.

Temporal Discretization The system (4) may be written as a system of ordinary differential equations

$$(5)\qquad \frac{d}{dt}\mathbf{u} = \mathbf{f}(t, \mathbf{u}),$$

where $\mathbf{u} \equiv (\mathbf{n}, \mathbf{w})^T$. The Adams fourth-order predictor-corrector scheme (P_4EC_4E) is used for the integration of (5) in time. The numerical scheme for $\mathbf{u}$ is

$$\begin{aligned}\tilde{\mathbf{u}}^{l+1} &= \mathbf{u}^l + \frac{\Delta t}{24}\big[55\mathbf{f}^l(\mathbf{u}^l) - 59\mathbf{f}^{l-1}(\mathbf{u}^{l-1}) + 37\mathbf{f}^{l-2}(\mathbf{u}^{l-2}) - 9\mathbf{f}^{l-3}(\mathbf{u}^{l-3})\big],\\ \mathbf{u}^{l+1} &= \mathbf{u}^l + \frac{\Delta t}{24}\big[9\mathbf{f}^{l+1}(\tilde{\mathbf{u}}^{l+1}) + 19\mathbf{f}^l(\mathbf{u}^l) - 5\mathbf{f}^{l-1}(\mathbf{u}^{l-1}) + \mathbf{f}^{l-2}(\mathbf{u}^{l-2})\big],\end{aligned}$$

where $\mathbf{f}^l(\mathbf{u}^l) = \mathbf{f}(l\Delta t, \mathbf{u}^l)$. In case the exact values of the boundary terms h_1', h_2', v_1' and v_2' in (4) are not available, they are calculated via the fourth-order central difference formula.

3 Existence of oscillatory waves of permanent form and their stability.

In paper [5], an exact oscillatory traveling-wave solution

$$(6)\qquad \begin{aligned}u_{ex}(x,t;x_0) &= \pm\frac{15}{2}\mathrm{sech}^2\left(\frac{3}{\sqrt{10}}(x - x_0 \mp \frac{5}{2}t)\right),\\ \eta_{ex}(x,t;x_0) &= \frac{15}{4}\left(2\mathrm{sech}^2\left(\frac{3}{\sqrt{10}}(x - x_0 \mp \frac{5}{2}t)\right) - 3\mathrm{sech}^4\left(\frac{3}{\sqrt{10}}(x - x_0 \mp \frac{5}{2}t)\right)\right),\end{aligned}$$

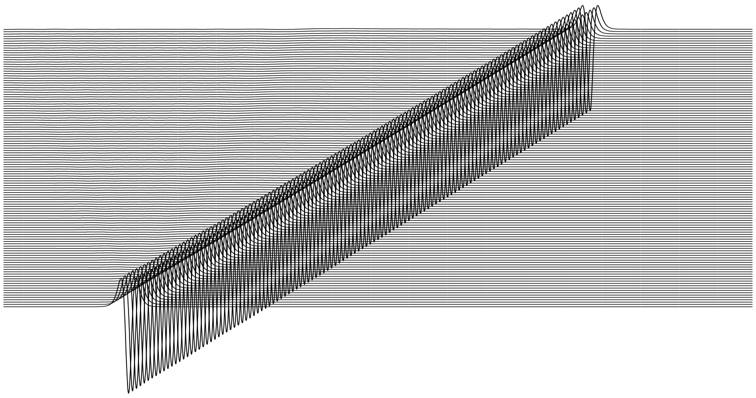

FIG. 1. *Overview of the wave profile*

which consists a big trough in the middle, a smaller crest in front the trough and another after the trough, was found. Solution (6) represents a zero-volume, namely $\int_{-\infty}^{+\infty} \eta_{ex} dx = 0$, traveling wave of permanent form. In this experiment, we subjected the exact solution to two kinds of disturbances and observed the evolution of the wave for a relatively long time interval. In both cases, we took $L = 800$, $\Delta x = \Delta t = 1/64$, and conducted the simulation for $t \in [0, 180]$.

In the first case, the perturbation on the exact solution is oscillatory and has a volume -0.0237. More precisely,

$$\begin{aligned} \eta_0(x) &= (1 + 0.01\sin(x))\eta_{ex}(x, 0; 240), \\ u_0(x) &= (1 + 0.01\cos(x))u_{ex}(x, 0; 240), \end{aligned}$$

was used as initial condition. An overview of the evolution is plotted in figure 1, which shows that a leading steady traveling wave followed by a small tail were developed as time evolves.

In figure 2, we compared the leading wave of the solution at $t = 180$ with the exact solution (6). The trough of the leading wave has a depth -3.544 which is not as deep as the one in (6), and the crests have a height 1.0265 which is about 82.1% of that in (6). The velocity profile of the leading wave is very close to that in (6). Based on the numerical data, we found that the phase velocity of the leading wave is approximately 2.4688 which is slight smaller than 2.5, the phase velocity of the exact solution. It is worth to note that the leading wave has a volume which equals to -0.41. Since our numerical computation preserves the mass conservation, which was confirmed throughout the computation, the tail part of the solution has a volume $0.41 - 0.0237 = 0.3827$.

A closer look of the tail (by stretching the y-axis) can be found in figure 3 which shows that the tail consists a leading solitary wave followed by a dispersive tail of an even smaller amplitude. The leading solitary wave can be understood by the positive volume of the tail, which is equal to 0.3827.

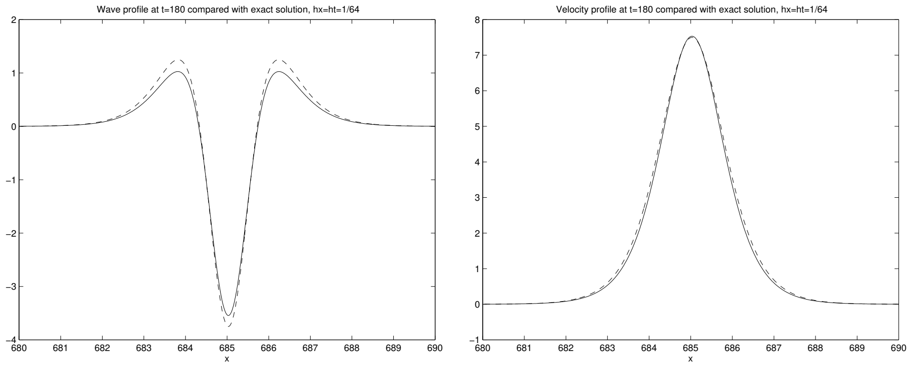

FIG. 2. *The leading wave profile of* (η, u) *at* $t = 180$ *(solid line) compared with (6) (dash line)*

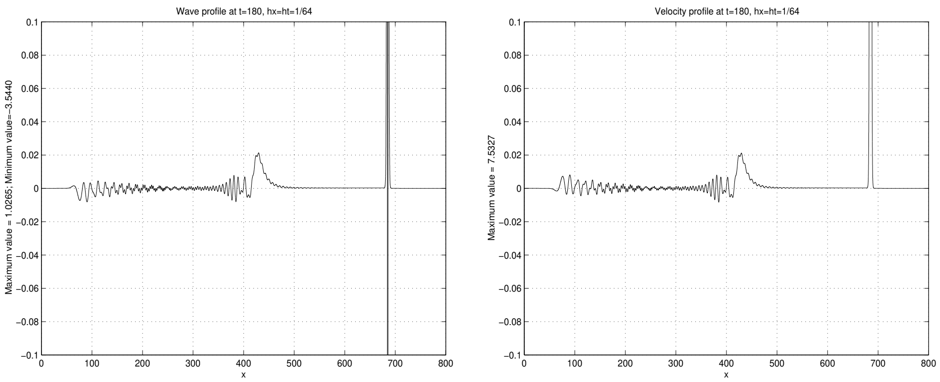

FIG. 3. *Wave and velocity profiles at* $t = 180$

In the second case, solution (6) was subjected to a volume-free disturbance, namely

$$
\begin{aligned}
\eta_0(x) &= (1 + 0.01)\eta_{ex}(x, 0; 240), \\
u_0(x) &= u_{ex}(x, 0; 240),
\end{aligned}
\tag{7}
$$

was used as initial data. Although the disturbance in this case is rather different from the one in the first case, it is worth to note that the solutions at $t = 180$ are very similar. The leading oscillatory wave developed in this case is almost identical to that in the first case.

References

[1] J. Thomas Beale, Thomas Y. Hou and John Lowengrub, *Convergence of boundary integral methods for water waves*, SIAM J. Numer. Anal, 33, 5 (1996), pp. 1797-1843.

[2] J. Bona and M. Chen, *A Boussinesq system for two-way propagation of nonlinear dispersive waves*, to appear in Physica D (1998).

[3] J. L. Bona, W. G. Pritchard and L. R. Scott, *An evaluation of a model equation for water waves*, Phil. Trans. Royal Soc. London A, 302 (1981), pp. 457-510.

[4] J. L. Bona, J. -C. Saut and J. F. Toland, *Boussinesq equations for small-amplitude long wavelength water waves*, preprint.

[5] M. Chen, *Exact Solutions of Various Boussinesq systems*, to appear in Appl. Math. Lett. (1998).

[6] G. B. Whitham, *Linear and nonlinear waves*, John Wiley & Sons: New York, (1974).